Supplemental Document

Journal of the Optical Society of America A
OPTICS, IMAGE SCIENCE, AND VISION

Quantifying CIE alpha-opic signals in the indoor built environment: supplement

Samuel Ponting,[1,*] Ruth Kelly Waskett,[2] Manuel Spitschan,[3,4] and Hannah E. Smithson[1]

[1] *Department of Experimental Psychology, University of Oxford, Oxford, UK*
[2] *Hoare Lea, London, UK*
[3] *Technical University of Munich, Munich, Germany*
[4] *Max Planck Institute of Biological Cybernetics, Tubingen, Germany*
[*] *samuel.ponting@pmb.ox.ac.uk*

Supplement DOI: https://doi.org/10.6084/m9.figshare.28381505

Parent Article DOI: https://doi.org/10.1364/JOSAA.545151

QUANTIFYING CIE ALPHA-OPIC SIGNALS IN THE INDOOR BUILT ENVIRONMENT: SUPPLEMENTAL DOCUMENT

Figure S1 contains information about the artificial lights in the scene. These lights are motion sensitive, turning on when movement in the office is sensed, regardless of ambient light level. Plots a) and b) show the spectrum and relative photoreceptor responses to the overhead lights. Plots c) and d) show the spectrum and relative photoreceptor responses to the light emitted by the screen throughout the duration of the experiment. Schematic e) shows a schematic of the office space, with the locations of the overhead lights shown in purple. Table f) shows chromatic information for each of the light types.

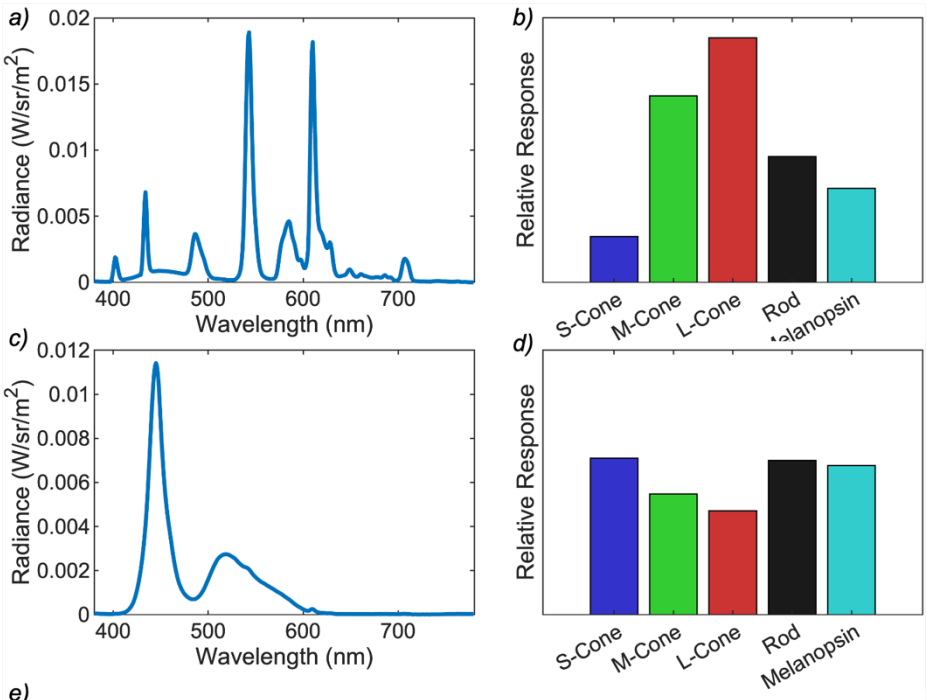

f)

	Room Lights	Monitor
Light Type	Fluorescent	LED
CCT	3337K	N/A
CIE 1931 xy	x = 0.4212	x = 0.1892
	y = 0.4110	y = 0.1960
Intensity	345 lux	97 cd/m²

Fig. S1. Schematic providing information about the artificial lights in the office space. a) shows the light spectrum emitted by the overhead lights, and b) shows the relative cone responses to this spectrum. c) shows the light spectrum emitted by the monitor, and d) shows the relative cone responses to this spectrum. e) shows a schematic of the office space, with the three purple bars denoting the locations of the lighting strips. f) is a table featuring additional colorimetric information about the lights. The intensity of the room lights is quantified in illuminance, measured from the desk in front of the camera. The intensity of the monitor is quantified in luminance.

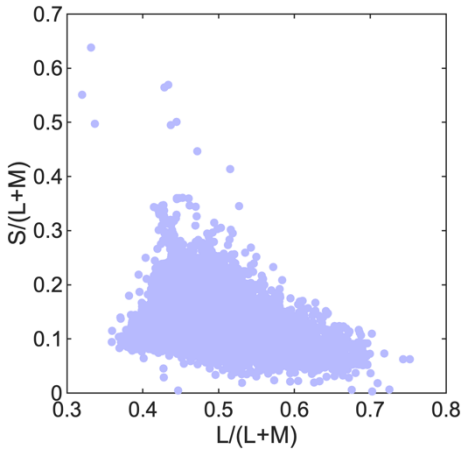

Fig. S2. Scatter plot showing the chromatic distribution of pixels in the indoor region under only artificial light, plotted in MacLeod-Boynton chromaticity space, where the x axis corresponds to L/(L+M), and the y axis corresponds to S/(L+M).

Figure S2 shows a scatter plot of the chromatic distribution of the indoor scene with artificial illumination. This data is taken from a sample from the January dataset after dusk, such that there was no light entering the scene via the windows, but the indoor lights and computer monitor were still on.

Figure S3 shows cartoon images of the view out of the North (plot a) and East (plot b) windows. The images are split into *sky* (blue), *foliage* (green), *building* (orange) and *tarmac* (black) sections. Where applicable, a sun path is shown. Specifically, the sun path is visible from the East window at around 07:00 each day in the May dataset.

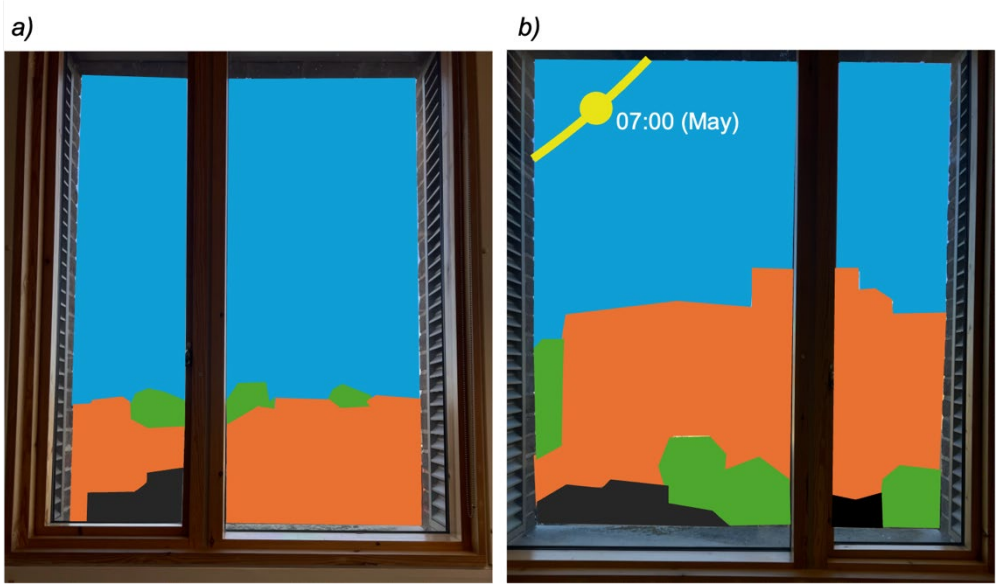

Fig. S3. Cartoon images of the terrain visible out of the North (a) and East (b) windows. The regions are categorised into sky (blue), buildings (orange), foliage (green) and tarmac (black).The East window shows a partial sun path in yellow, with the sun being directly visible at 07:00 each day of the May dataset. It was not directly visible in January.

Figure S4 has the same data structure as Figure 5, but for luminance-weighted chromaticity statistics. Here, each datapoint relates to a statistic averaged across the region defined at the top of each column, weighting pixels within the region based on their L+M value. Similar results are observed from these data as were observed in the non-luminance weighted data – the May dataset shows a 'greening' compared to the January dataset, such that L/(L+M) statistics decrease, while I/(L+M) and S/(L+M) statistics increase. However, the spread of differences is different for this data. Notably, differences in the 'whole image' datapoints are greatly reduced,

while differences in the 'window' datapoints are increased. Kruskal-Wallis tests were also conducted for this data, the results of which are shown in Table S1.

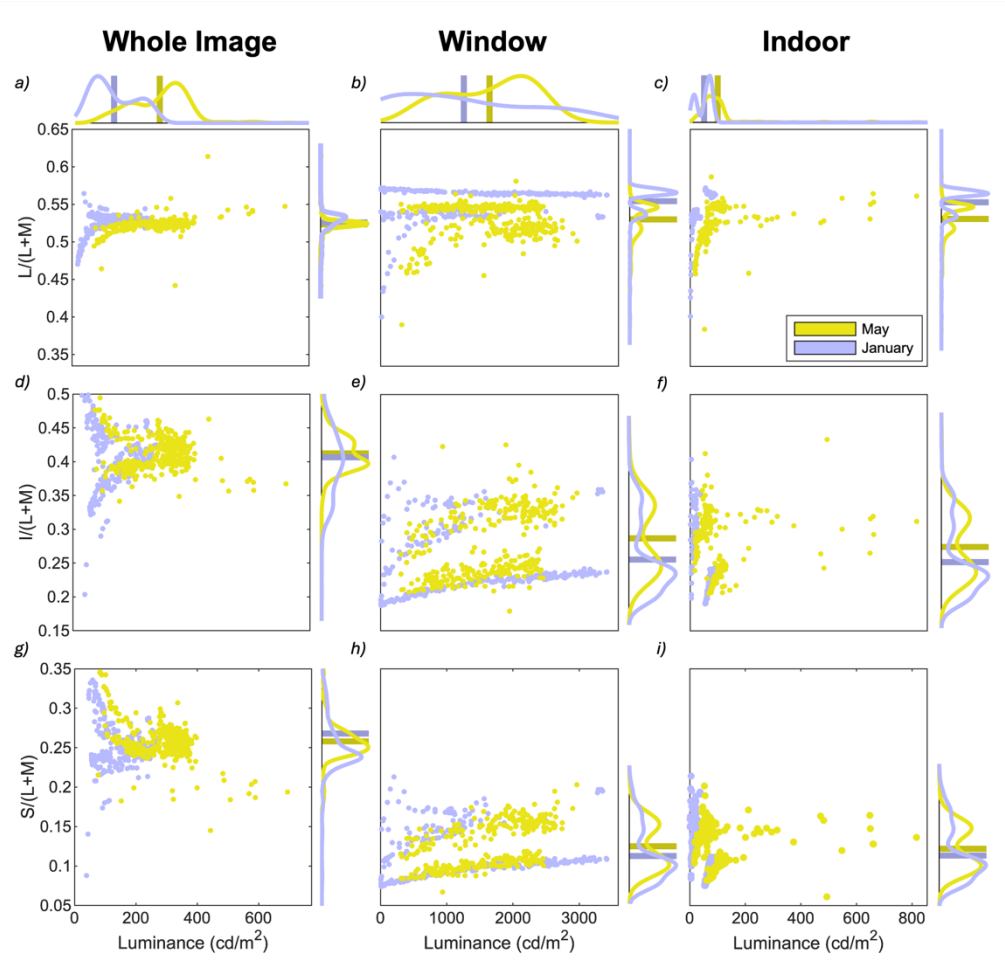

Fig. S4. Scatter plots and histograms for luminance-weighted mean chromatic and luminance values across different regions comparing the January and May datasets. January data are shown in blue, and May data in yellow. Each subplot shows a scatter plot and two kernel-smoothed histograms showing the distribution of each variable. Darkened bars on the histograms denote the mean for each variable. The left column shows whole image data, the middle column shows the window region data, and the right column shows the indoor region data. The top row shows L/(L+M) statistics, the middle row shows I/(L+M) statistics and the bottom row shows S/(L+M) statistics.

Table S1. Luminance-weighted Kruskal-Wallis test statistics for seasonal differences

		Luminance	*L/(L+M)*	*I/(L+M)*	*S/(L+M)*
Whole Image	χ^2	257.76 +	1.97	42.68 +	26.4 -
	p	**<.001**	.160	**<.001**	**<.001**
Window	χ^2	30.21+	29.29	40.32 +	12.84 +
	p	**<.001**	**<.001** -	**<.001**	**<.001**
Indoor	χ^2	153.14 +	25.26	18.55 +	4.12 +
	p	**<.001**	**<.001** -	**<.001**	**.0423**

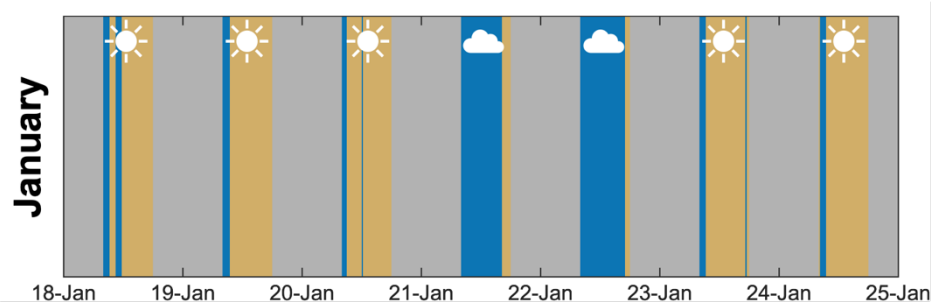

Fig. S5. Timeseries plots where timepoints are colour-coded by the polarity of the difference in L/(L+M) between the window and indoor regions. Timepoints before sunrise and after sunset are coloured grey. Orange timepoints indicate a time where L/(L+M) was lower in the window region than the indoor region, and blue timepoints indate that L(L+M) was higher in the window region compared to the indoor region. White weather icons denote the weather grouping for each day.

Figure S5 shows a timeseries plot for the January dataset, where timepoint data are grouped based on whether the difference in L/(L+M) between the indoor and window regions was positive or negative (see Fig. 4). Orange timepoints indicate that the window L/(L+M) is lower than the indoor L/(L+M), while blue timepoints indicate that the window L/(L+M) is higher.

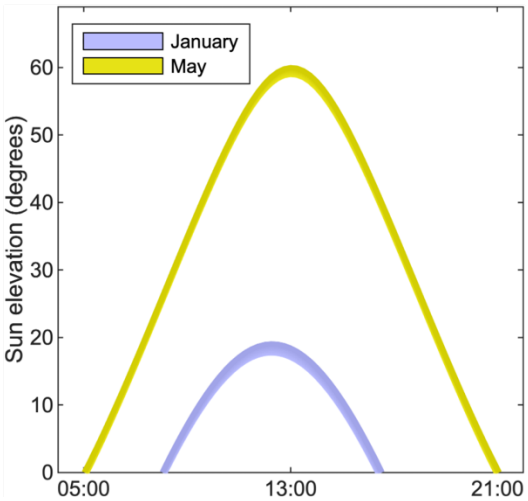

Fig. S6. Sun elevation angles for January and May datasets at the geographic location of the test site (51.76° N, -1.27° W) across the daytime samples. January data are shown in blue and May data are shown in yellow.

Figure S6 shows the sun elevation angle throughout the daytime period in each data capture sequence. There is a marked difference in the range of daytime sun elevations across different seasons, with the highest elevation angles in January being greatly reduced to those observed in May.

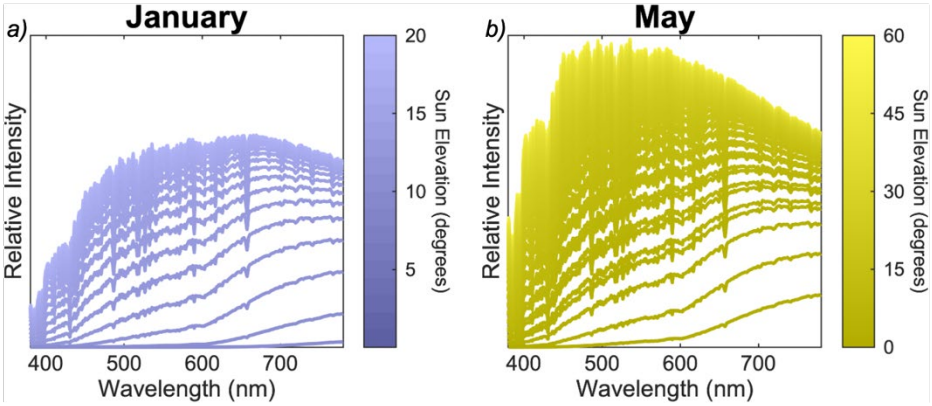

Fig. S7. Spectral plots of modelled daylight spectra [33]. Left figure shows January data, and right figure shows May data. Spectra lines are colored according to the sun elevation, shown by the color bars to the right of each plot.

Figure S7 shows the range of modelled sun spectra for the January and May datasets respectively, modelled in Smithson et al. (2014) [33]. The model considers the effect of Rayleigh scattering, aerosol scattering, Ozone Chappuis band absorption and sun elevation on the observed sun spectrum. The model does not account for molecular oxygen and water vapor absorption. Spectra are colored according to their respective sun elevation. The May dataset shows increased intensity, particularly in shorter wavelengths.

Figure S8a shows the chromaticity of the spectra plotted in S7 in a MacLeod-Boynton chromaticity diagram. Datapoints are colored according to their respective sun elevation. Black lines join datapoints from the same time of day (e.g., a datapoint from 9:00am in January and 9:00am in May). Different day lengths mean these timepoints have different sunlight chromaticities. Chromaticities corresponding to the sun elevation during May dataset are greener and bluer than the chromaticities from January. Figure S8b shows the size and direction of these differences, with each line coloured according to its time of day. The largest chromatic differences occur early and late in the day, with the smallest differences occurring at 12:15.

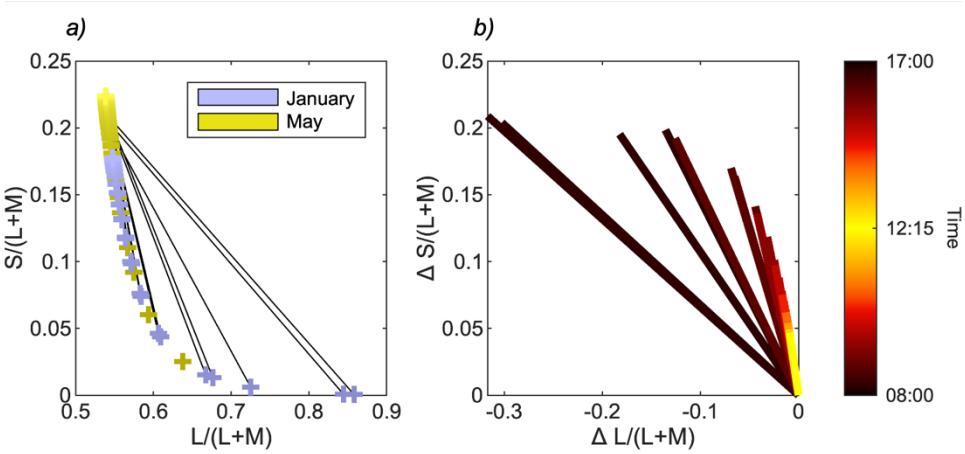

Fig. S8. a) Chromaticity plot of modelled sunlight spectra across January and May datasets. January data are plotted in blue and May data are plotted in yellow. Datapoints are darkened based on their corresponding sun elevation. Black lines join datapoints taken from the same hour of day. b) Difference vectors connecting chromaticities from the same time of day in January and May. Lines are coloured according to their time of day.

We have additionally investigated environmental signals for the decorrelation between S-cone and melanopic light intensity. Figure S9 shows the Spearman's Rho statistics for correlations between S-cone intensity and melanopic light intensity across regions and seasons, with darker and lighter lines representing overcast and sunny day data, respectively. In all cases, S and I are highly correlated, and differences between regions, seasons and weather conditions are minimal. However, correlation statistics are notably reduced at sunrise in the window and indoor regions. This reflects times in which there are greater directional light signals due to the lowered sun elevation.

Figure S10 shows Spearman's Rho statistics for correlations between luminance and different chromatic statistics within the indoor region. Here the data are split into 'sunny' and 'overcast'

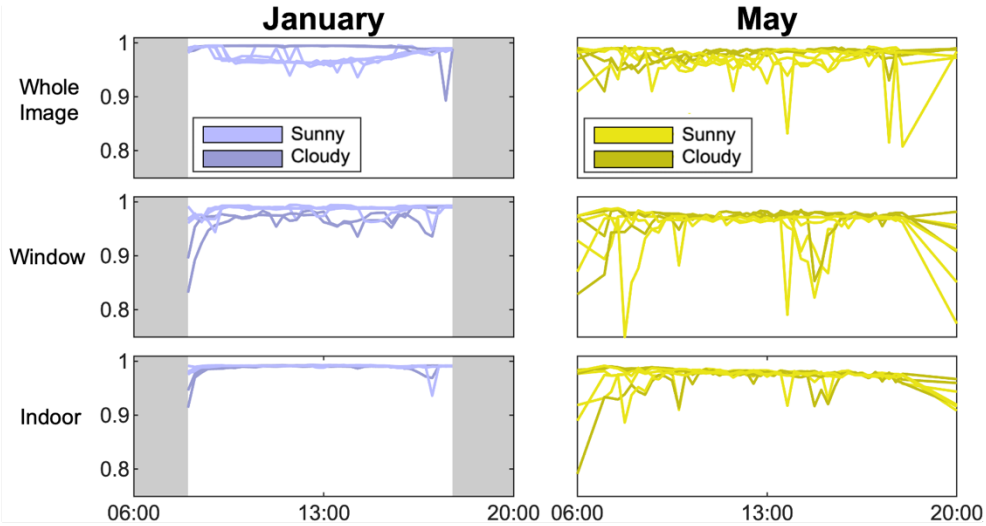

Fig. S9. Spearman's Rho statistics for correlations between S-cone intensity and melanopic intensity across different regions and seasons, and in different weather conditions. Overcast days are shown in darker colours, and sunny days in lighter colours. The grey shading appears before sunrise and after sunset.

days based on the data in Figure 7. 'Sunny' day data are shown in light colours, and 'overcast' day data are shown in dark colours. Throughout both datasets, and in both weather conditions, L/(L+M) has a positive relationship with luminance, such that pixels with higher intensity contain more long-wavelength light. However, both season and weather have different effects on the shorter-wavelength dependent statistics. In the January dataset, 'sunny' days show a persistent negative relationship between luminance and these statistics, while 'overcast' days show a relationship close to 0 in the mornings, which decreases throughout the day. In the May dataset, 'sunny' days also show less correlation than cloudy days, with S/(L+M) being more

strongly negative than I/(L+M). ‘Overcast’ days in May show less variation than ‘overcast’ days in January, having a consistent positive relationship for both statistics.

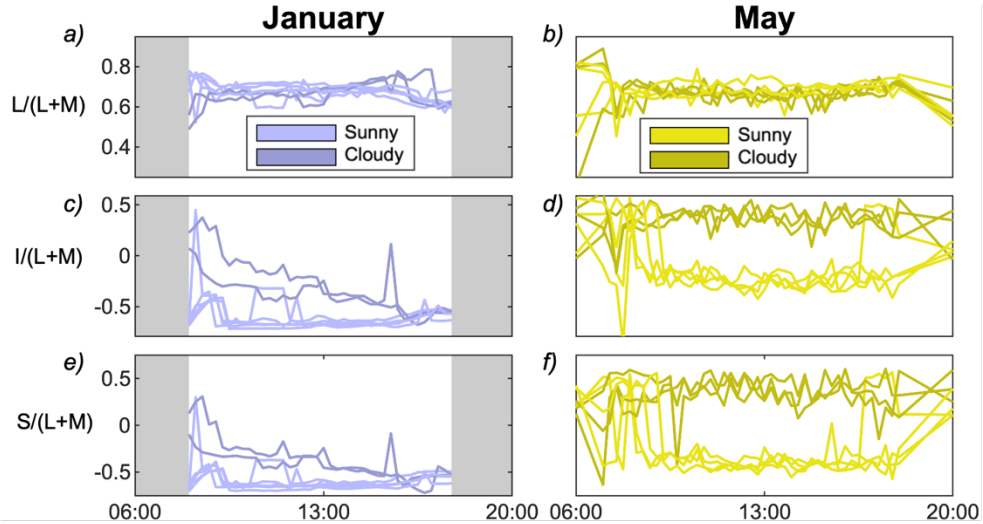

Fig. S10. Spearman’s Rho statistics for correlations between chromatic statistics and luminance for pixels within the indoor region, averaged across specific days within the 7-day capture period. Each subplot shows a combination of season and chromatic statistic, where the left column shows correlations in January and the right column shows correlations in May. The top row shows correlations between luminance and L/(L+M), the middle row shows correlations between luminance and I/(L+M) and the bottom row shows correlations between luminance and S/(L+M). Within each plot, the light-coloured lines show data for the ‘sunny’ days, and the dark-coloured lines show data for the ‘overcast’ days. The grey shading appears before sunrise and after sunset.